Ionic Conductivity of $Li_{1+x}Ti_2(PO_4)_3$ ($0.2 \leq x \leq 1.72$) with NASICON-Related Structures

B. Wang and M. Greenblatt*

Department of Chemistry, Rutgers—The State University of New Jersey, Piscataway, New Jersey 08855-0939

S. Wang and S.-J. Hwu

Department of Chemistry, Rice University, P.O. Box 1892, Houston, Texas 77251

Received August 14, 1992. Revised Manuscript Received October 26, 1992

Introduction

Recently, lithium ion conductors based on $Li(M^{IV})_2(PO_4)_3$ with M = Ti^{IV}, Zr^{IV}, and Hf^{IV} have attracted interest.[1-5] These compounds are structurally related to solid solution of NASICON, $Na_{1+x}Zr_2P_{3-x}Si_xO_{12}$. The structure of the NASICON-related phosphate compounds is characterized by $M_2(PO_4)_3$ units of corner-sharing MO_6 octahedra and PO_4 tetrahedra. These basic structural units join by additional corner sharing to form a three-dimensional (3D) framework structure. The mobile cations are distributed in the three-dimensionally connected channels of the network structure. High lithium ion conductivities have been observed in these NASICON-related phosphate solid solutions. For example, the conductivity in the $Li_{1+x}(Ti^{IV})_{2-x}(In^{III})_x(PO_4)_3$ series is 5.5×10^{-2} S/cm at 300 °C for $x = 0.4$,[1] an order of magnitude lower than the highest conductivity in NASICON.

Recently, the structure of a new series of lithium titanium (III/IV) phosphates, $Li_{1+x}Ti_2(PO_4)_3$ ($0 \leq x \leq 2$), has been systematically studied.[6,7] Both the $x = 0.78$ and the $x = 1.72$ compounds form a frameworks structure built from $Ti_2(PO_4)_3$ units which contain large NASICON-like channels. In both compounds there are two different channel geometries along the [100] direction: one is characterized by large pseudopentagonal windows and the other by small octagonal windows (Figure 1). The pentagonal channels are partially occupied by the Li ions (i.e., clearly, the occupancy changes with x), while the smaller octagonal channels in Figure 1 are empty. The pentagonal "windows" are significantly larger than 2 times the Li–O distance.

The structure of the series varies significantly for $0 \leq x \leq 2$.[6,7] The most notable difference is the connectivity of the $Ti_2(PO_4)_3$ units. For example, in the $x = 0.78$ phase, the framework consists of double $Ti_2(PO_4)_3$ units that share corner oxygen atoms as shown in Figure 2a. The double units are connected so that two different "cage" sizes: 3 octahedra + 3 tetrahedra (3O + 3T) and 4 octahedra + 4 tetrahedra (4O + 4T) are found in a single slab plane. These cavities are fully occupied by Li ions. Li ions in the pentagonal "channel" sites have 11 nearest oxygen neighbors, while those in the "cage" sites have 6 oxygen coordination. These two sites are interconnected by various "windows" formed by oxygens, which are commonly shared by the center of two sites. The size of these "windows" is determined by the structure type (i.e., I, II, or III). Thus the various cavities are interconnected in three dimensions, and because some of them are only partially occupied, Li^+ mobility is facilitated. Slab structures with a similar perspective as that given for $x = 0.78$ are shown for $x = 0.0$ and $x = 1.72$ in parts b and c of Figure 2, respectively. It is clear that the number of large voids (4O + 4T) decreases as the concentration of lithium increases. It was interesting to see how the ionic transport is affected by the various structural (i.e., ratio of large/small voids) and electronic effects (i.e., increasing Ti^{III}/Ti^{IV}) as x increases.

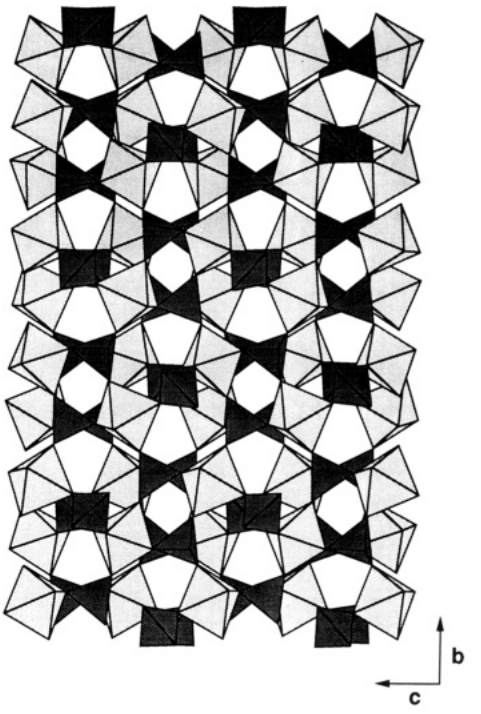

Figure 1. Structure of $Li_{1.78}Ti_2(PO_4)_3$ viewed along a.

In this paper we present results of the investigation of ionic conductivity for $0.2 \leq x \leq 1.72$ in $Li_{1+x}Ti_2(PO_4)_3$.

Experimental Section

High-purity, polycrystalline samples of the series $Li_{1+x}Ti_2(PO_4)_3$ ($0.2 \leq x \leq 1.72$) were synthesized by stoichiometric reactions from the reduced systems, Li_2O–TiO_z–P_2O_5 ($z < 2$), using procedures that were previously described.[6,7]

Powder X-ray diffraction (PXRD) patterns of the resulting samples were recorded at room temperature on a Philips PW

* To whom correspondence should be addressed.

(1) Li, S.; Lin, Z. *Solid State Ionics* **1983**, *9*, 835.
(2) Lin, Z.; Yu, H.; Li, S.; Tian, S. *Solid State Ionics* **1986**, *18*, 549.
(3) Subramanian, M. A.; Subramanian, R.; Clearfield, A. *Solid State Ionics* **1986**, *18*, 562.
(4) Hamdoune, S.; Tranqui, D. *Solid State Ionics* **1986**, *18*, 587.
(5) Tranqui, D.; Hamdoune, S.; Soubeyroux, J. L.; Prince, E. *J. Solid State Chem.* **1988**, *72*, 309.
(6) Wang, S.; Hwu, S.-J. *J. Solid State Chem.* **1991**, *90*, 377.
(7) Wang, S.; Hwu, S.-J. *Chem. Mater.* **1992**, *4*, 589.

0897-4756/93/2805-0023$04.00/0

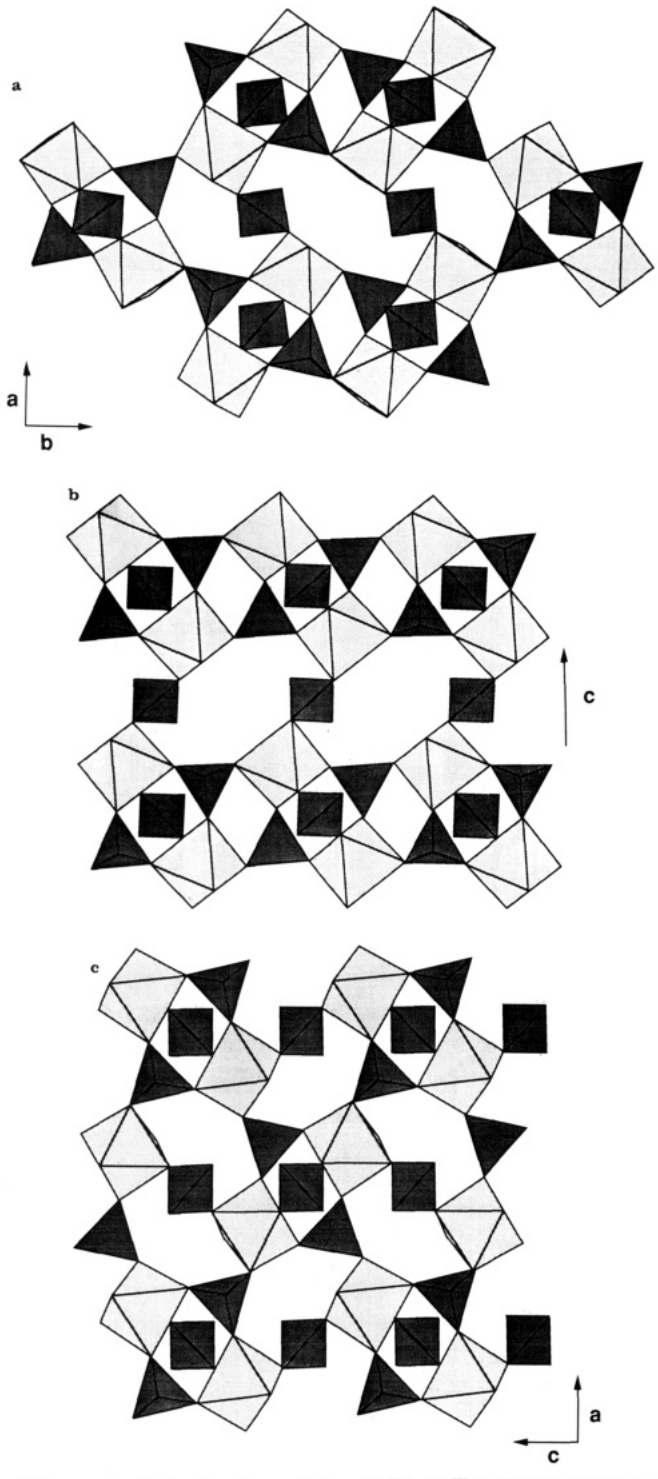

Figure 2. Slab structure of $Li_{1+x}Ti^{IV}_{2-x}Ti^{III}_{x}(PO_4)_3$ for (a) x = 0.78 projected along c, (b) x = 0 (NASICON phase) projected along b, and (c) x = 1.72 projected along b.

1840 diffractometer with Ni-filtered Cu Kα radiation. The PXRD patterns ($5° \leq 2\theta \leq 60°$) were indexed and the cell constants were refined by the program POLSQ.[8] Differential thermal analysis (DTA) was carried out with a Du Pont Model 9900 thermal analyzer with a heating rate of 2 °C/min in flowing helium.

Ionic conductivities were measured by an ac complex impedance technique with a Solartron Model 1250 frequency analyzer and 1186 electrochemical interface that were programmed by a Hewlett-Packard 9816 desktop computer for data collection and analysis. Samples were pelletized and coated with platinum paste.

(8) Keszler, D.; Ibers, J. POLSQ, FORTRAN program; Northwestern University, 1983.

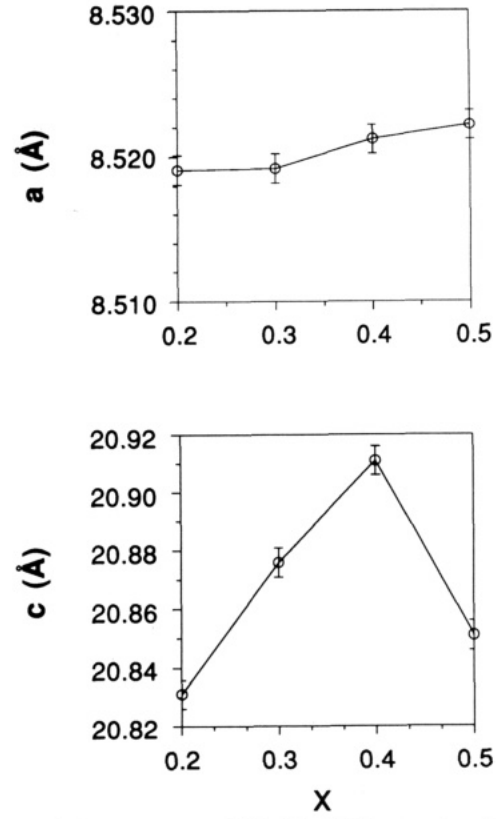

Figure 3. Cell parameter of $Li_{1+x}Ti_2(PO_4)_3$ as a function of x ($0.2 \leq x \leq 0.5$).

The frequency range 10 Hz to 65 kHz was employed at a heating rate 2 °C/min in the temperature range 25–400 °C in flowing helium.

Results and Discussion

Structural studies show that the $Li_{1+x}Ti_2(PO_4)_3$ compounds adopt, depending on the x value, three structure types: phase I, $0.0 \leq x \leq 0.5$, is rhombohedral, $R\bar{3}c$; phase II, $0.50 < x < 1.20$, is orthorhombic, *Pbca*; and phase III, $1.20 \leq x \leq 2.00$, is orthorhombic, *Pbcn*.[6,7] In contrast to NASICON, the transitions from phase I to phase II and from phase II to phase III result in structural changes of the framework. As we have discussed above, the rhombohedral $R\bar{3}c$ structure (phase I) is of the NASICON type (Figure 2b). The building blocks of these NASICON structures consist of PO_4 tetrahedra from adjacent slabs and infinite $[Ti_2(PO_4)_3]_\infty$ chains (Figure 2b). In the orthorhombic *Pbca* phase II, which is represented by $Li_{1.78}Ti_2(PO_4)_3$, the framework consists of double $Ti_2(PO_4)_3$ units that share corner oxygen atoms, as shown in the slab structure (Figure 2a). In the orthorhombic *Pbcn* phase III, which is represented by $Li_{2.72}Ti_2(PO_4)_3$, the building blocks consist of PO_4 tetrahedra from adjacent slabs and single $Ti_2(PO_4)_3$ groups (Figure 2c). Throughout the structural changes from phase I through phase II to phase III, the basic $Ti_2(PO_4)_3$ structural unit is conserved. A comparison of these structures shows that the number of large voids (characterized by 4O + 4T), which are the characteristic voids in the x = 0, NASICON phase, decrease as the lithium concentration increases and are completely replaced by the smaller voids defined by 3O + 3T at x = 2.

Figure 3 shows the cell parameters as a function of x for the NASICON-type structure ($0.2 \leq x \leq 0.5$). The cell parameters are expected to increase with x, since the

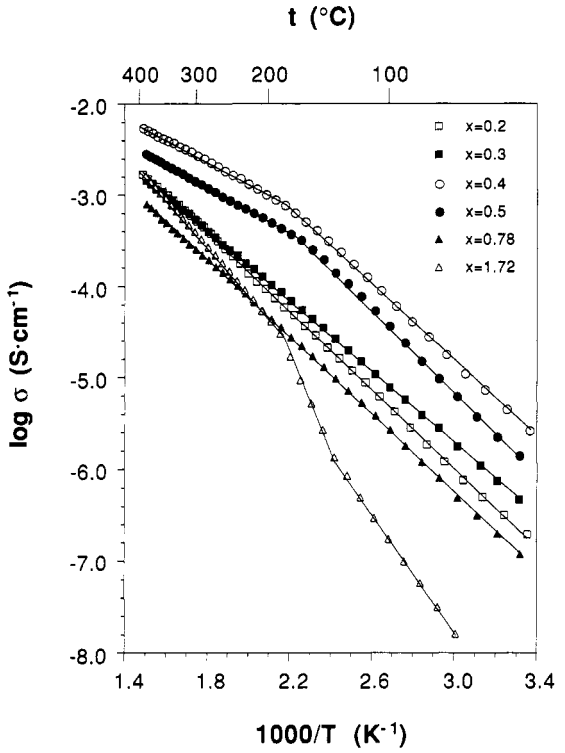

Figure 4. Arrhenius plots of conductivity of $Li_{1+x}Ti_2(PO_4)_3$.

Table I. Conductivity Data of $Li_{1+x}Ti_2(PO_4)_3$

x	E_a (eV)	$\sigma_{300°C}$ (S cm^{-1})
0.2	0.42	5.0×10^{-4}
0.3	0.38	5.2×10^{-4}
0.4	0.42,[a] 0.24[b]	2.7×10^{-3}
0.5	0.45,[c] 0.25[d]	1.4×10^{-3}
0.78	0.42	2.6×10^{-4}
1.72	0.64,[e] 1.00,[f] 0.52[g]	3.8×10^{-4}

[a] 25–190 °C. [b] 190–400 °C. [c] 25–170 °C. [d] 170–400 °C. [e] 25–140 °C. [f] 140–190 °C. [g] 190–400 °C.

effective ionic radius of Ti^{III} (0.810 Å) is larger than that of Ti^{IV} (0.745 Å).[9] The decrease in the c parameter at x = 0.5 could be due to change in the structure. The x = 0.5 sample can be indexed on the *Pbca* orthorhombic structure (i.e., there are extra lines with respect to the rhombohedral, $R\bar{3}c$ space group). The cell parameters of $x > 0.5$ phases are omitted, because they form with different structures and have much lower conductivities.

Arrhenius plots of the ionic conductivity of these compounds are displayed in Figure 4. The log conductivity (σ) vs $1/T$ plots fall into three categories: (1) a straight line for x = 0.2, 0.3, and 0.78, (2) a change of slope around 180 °C for x = 0.4 and 0.5, and (3) a discontinuity at 140–190 °C for x = 1.72. The calculated activation energies and conductivities at 300 °C for these samples are listed in Table I.

The discontinuity in the conductivity for the x = 1.72 sample is also seen at around 150 °C in the differential thermal analysis (DTA). An endotherm in the DTA at 158 °C in Figure 5 is confirmation of a phase transition although high temperature X-ray powder pattern shows no significant change from the room temperature pattern. This phase transition might be due to a redistribution of the mobile lithium ions moving in-and-out of the different interstitial sites reversibly, when the thermal distortion of the framework takes place at the transition temperature.

(9) Shannon, R. D. *Acta Crystallogr.* **1976**, *A32*, 751.

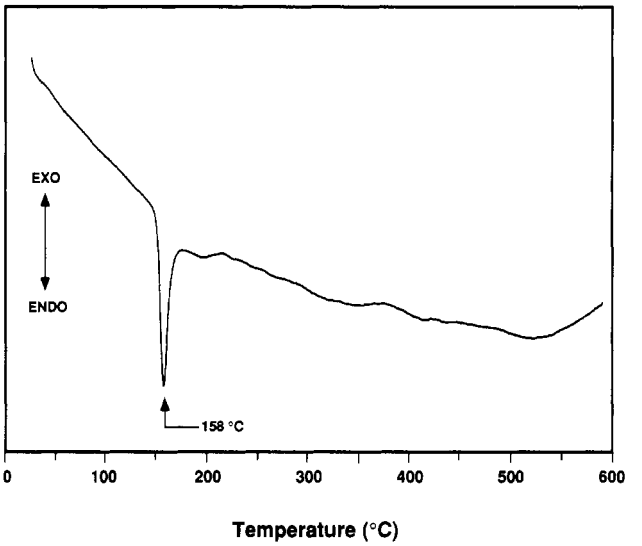

Figure 5. Differential thermoanalysis (DTA) of $Li_{2.72}Ti_2(PO_4)_3$ with a heating rate of 2 °C/min.

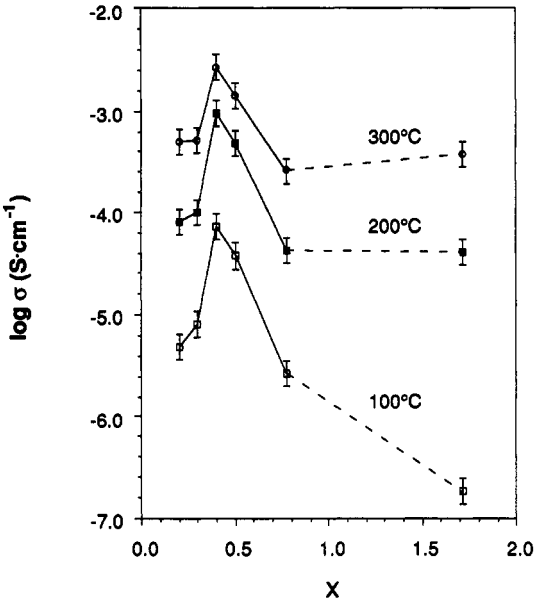

Figure 6. Isotherms of the conductivity in $Li_{1+x}Ti_2(PO_4)_3$.

The change in the slope of the Arrhenius plots of x = 0.4 and 0.5 samples may be associated with long range lithium motion. The anomaly seen in the log σ vs $1/T \sim$ 180 °C (Figure 4) was not observed by either DTA or high-temperature X-ray powder diffraction. A similar result was observed in $LiZr_2(PO_4)_3$, where the structure remains rhombohedral above the transition temperature.[10]

The conductivity isotherms of $Li_{1+x}Ti_2(PO_4)_3$ at 100, 200, and 300 °C, as a function of x are shown in Figure 6. Figures 4 and 6 both indicate that the conductivity increases with increasing x to a maximum at x = 0.4 and then decreases with further increasing x. Figure 7 shows the variation of activation energy E_a (between 25 and 140 °C) and preexponential factor A as a function of x (i.e., E_a and A defined by the Arrhenius equation $\sigma = A \exp(-E_a/RT)$).

A comparison of Figures 6 and 7 shows that the increase of conductivity for $x < 0.3$ is due to the combined effect of decreasing activation energy and increasing preexpo-

(10) Petit, D.; Colomban, Ph.; Collin, G.; Boilot, J. P. *Mater. Res. Bull.* **1986**, *21*, 365.

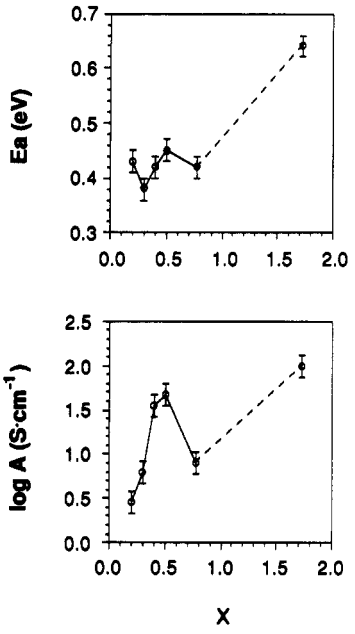

Figure 7. (a, top) Activation energy (E_a, 25–140 °C) vs x in $Li_{1+x}Ti_2(PO_4)_3$. (b, bottom) Preexponential factor (A, 25–140 °C) vs x in $Li_{1+x}Ti_2(PO_4)_3$.

nential factor. The decrease of E_a in this region can be ascribed to the increase in the "bottleneck" size for lithium migration, as evidenced by the increase in the unit-cell parameters with increasing x (Figure 3). The increase in the preexponential factor is probably due to a larger concentration of mobile cations. For $x > 0.3$, the increase in E_a is attributed to stronger Li–O interactions in the structure with increasing concentration of the less electronegative Ti^{III} ions substituted for Ti^{IV}. Since Ti^{IV} is more electronegative than Ti^{III} (1.577 and 1.414 for Ti^{IV} and Ti^{III}, respectively[11]), one expects the Ti^{IV}–O bond to be more covalent (less ionic) than the Ti^{III}–O bond. Consequently, the Li^+–oxygen bond in Li–O–Ti^{III} should be stronger than in Li–O–Ti^{IV}. Thus the electronegativity factor is expected to decrease the ionic conductivity in the Ti^{III}-substituted phases. The increasing occupancy of sites also contributes to the increase of activation energy. On the other hand, the increase in the preexponential factor (Figure 7b) is ascribed to the increasing Li^+ ion concentration with increasing x. It appears that the observed increase of conductivity for $x > 0.3$ is dominated by the increasing preexponential factor.

For $0.5 < x \leq 0.78$, both the activation energy and preexponential factor decrease with increasing x. A comparison of Figures 6 and 7 suggests that the conductivity is more strongly affected by the decreasing preexponential factor than by the decreasing activation energy in this region. The decreasing activation energy is probably due to the ordering of Ti^{III} and Ti^{IV} in phase II, which is characterized by a doubling of the longest axis in the x = 0.78 structure.[7] In phase I, Ti^{III} and Ti^{IV} are randomly distributed in the octahedral sites. The separation of Ti^{III} and Ti^{IV} probably results in a weakening of the Li–O interactions in the structure. This effect is stronger than the electronegativity effect and results in the observed decrease of E_a. In the x = 0.78 phase the occupancy of the pentagonal channels increases and the concentration of the larger "cages" decreases; the former leads to less available sites for Li^+ motion, the latter for the decrease of "window" size between the fully occupied "cage" sites and empty channel sites. These two effects lead to an apparent decrease of preexponential factor, which suggest that the number of mobile cations are actually decreasing for $x > 0.5$. The large decrease in A with increasing x in this range leads to the decrease of conductivity observed (Figures 6 and 7).

Both the activation energy and preexponential factor increase with increasing x for $0.78 < x \leq 1.72$. The large increase of E_a dominates the conductivity in this region (Figure 6). Several factors contribute to the increase of E_a in this region. Probably, the most important factor is the complete disappearance of the large voids (Figure 2c) in this structure. The "window" between the smaller, fully occupied "cage" sites and the partially occupied pentagonal, "channel" sites is considerably smaller in this case; moreover, there are fewer empty sites for Li^+ motion. In addition, the activation energy is expected to increase due to stronger Li–O interactions with increasing concentration of the less electronegative Ti^{III} ions substituted for Ti^{IV}. On the other hand, the increase in the preexponential factor (Figure 7b) is ascribed to the increasing Li^+ ion concentration with increasing x for $0.78 < x \leq 1.72$.

A comparison of the conductivity of the three phases indicates that the highest conductivity for $Li_{1+x}Ti_2(PO_4)_3$ is found for compounds with the NASICON structure. Similar results were observed in $Li_{1+x}(Ti^{IV})_{2-x}(M^{III})_x(PO_4)_3$ (M^{III} = Ga^{III}, In^{III}) with a maximum in conductivity at $x \sim 0.4$ (5).[5]

Conclusions

In $Li_{1+x}Ti_2(PO_4)_3$ ($0.0 \leq x \leq 0.5$) with the NASICON structure, the ionic conductivity can be enhanced by substituting small amounts of Ti^{III} for Ti^{IV}. The highest ionic conductivity was found in $Li_{1.4}Ti^{IV}_{1.6}Ti^{III}_{0.4}(PO_4)_3$ with the $\sigma \sim 2.7 \times 10^{-3}$ S/cm at 300 °C. The much lower conductivity of $Li_{1.78}Ti_2(PO_4)_3$ and $Li_{2.72}Ti_2(PO_4)_3$ is ascribed to changes in the network structure that lead to a decrease of the concentration of large voids in the structure with increasing x (i.e., no large voids at x = 1.72). Because the "window" for mobility diminishes between the occupied small "cage" cavities relative to the large "cage" sites, this structural change is clearly deleterious for Li diffusion. Furthermore, with increasing x, the concentration of Ti^{III} increases and because of the lower electronegativity of Ti^{III} vs Ti^{IV}, the Li–O interactions in the channel become stronger, which also leads to a lowering of the conductivity.

(11) Zhang, Y. *Inorg. Chem.* **1982**, *21*, 3886.